EasyChair Preprint

№ 1897

Stabilization of unstable limit cycles in a push-off based dynamic walker by reversible switching surfaces

Rana Danesh, Ali Tehrani Safa and Mahyar Naraghi

November 8, 2019

Stabilization of Unstable Limit Cycles in a Push-off Based Dynamic Walker by Reversible Switching Surfaces

Rana Danesh
Mobile Robots Research Lab, Mechanical Eng Dept.
*Amirkabir University of Technology**
Tehran, Iran
ranadanesh1371@aut.ac.ir
* MSc student, Amirkabir University of Technology

Ali Tehrani Safa
Mobile Robots Research Lab, Mechanical Eng Dept.
*Amirkabir University of Technology**
Tehran, Iran
atehranisafa@gmail.com
* Research assistant

Mahyar Naraghi
Mobile Robots Research Lab, Mechanical Eng Dept.
*Amirkabir University of Technology**
Tehran, Iran
naraghi@aut.ac.ir
* Associate Professor, Amirkabir University of Technology

***Abstract*—By employing the concept of "Reversible Switching Surfaces" (RSS), we demonstrate that it is possible to stabilize unstable periodic orbits of a push-off based dynamic walker. The concept is implemented by a simple event-based control which kinematically controls the foot during the swing phase to adjust the heel-strike. The feedback controller is designed based on the theory of Virtual Holonomic Constraints (VHC). Simulation results demonstrate, there exists a broad range of VHC which satisfies stable dynamic walking.**

***Index Terms*—dynamic walking, stability, reversible switching surfaces, virtual holonomic constraints**

I. Introduction

Due to human locomotion complexity, bipedal robots have not precisely presented human walking behavior. For instance, the robots based on "Zero Moment Point" (ZMP) are stable, but not sufficiently efficient [1], [2]. On the other hand, limit cycle walkers show efficient and human-like behavior; though, they do not have enough stability and robustness [3]–[6].

In order to solve the stability problem, researchers have suggested various solutions such as adding springs [7] and dampers [8], using upper body [9] or employing leg retraction method [10].

Safa proposed the theory of local slopes in 2016 [11]. He showed that it is possible to improve the stability of a passive dynamic walker by placing the robot on a terrain that is a combination of ramps and stairs. Further development of this theory resulted in the concept of Reversible Switching Surfaces (RSS) which has been used to design an efficient controller to stabilize the unstable periodic motions of a passive dynamic walker. This concept is defined as follows: (i) The system's switching surface replaces by a new one if an external disturbance is induced. (ii) The new switching surface is reshaped back into its old style, together with the disturbance rejection. (iii) The stabilization procedure is performed with as small energy consumption as possible [12].

In our previous study, we have shown the possibility of stability enhancement of a dynamic walker traversing a sloped surface [12]. This improvement was performed by a feedback controller, which kinematically controls the robot's flat feet during the swing phase. A "Virtual Holonomic Constraint" (VHC) [13] is designed for the feedback law. VHC has been widely used for several control problems including Furuta pendulum [14], pendubot [15], camless combustion engines [16], bicycles [17], and bipeds [18].

In this paper, we use the concepts of RSS and VHC to stabilize unstable limit cycles of a push-off based dynamic walker. Although this robot can walk on the level ground without any feedback control, the stability is not entirely guaranteed. Here, we reexamine RSS to show its effectiveness on the stability improvement of dynamic walking. In this regard, it has been shown that our curved feet dynamic biped can stably walk with longer step sizes at higher speeds.

The rest of the paper is organized as follows. Section II describes the bipedal walking model. Section III presents the simulation outputs, and Section IV concludes the paper.

II. The Bipedal Walking Model

Fig. 1 shows the bipedal walking model. The model consists of a point mass at the hip (shown by M), two infinitesimal point masses at the ankles (shown by m), massless legs and curved feet. The bouncing, slipping, double supporting, and foot scuffing are neglected. All joints are frictionless, and the impacts are assumed to be perfect plastic. Also, the foot length is assumed to be large enough to avoid the rotation around the heel or toe during the stance phase.

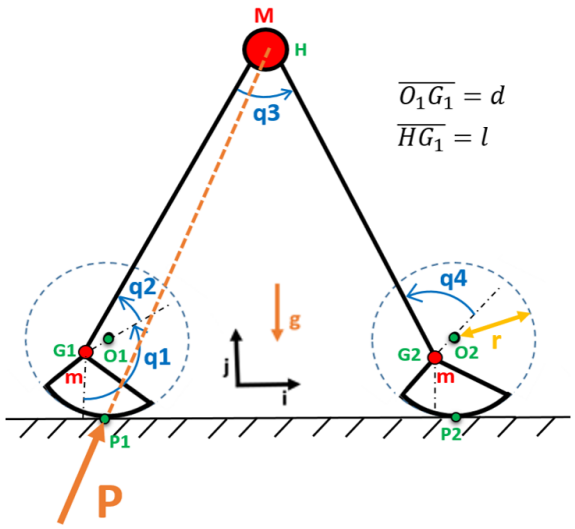

Fig. 1. Parameters and variables of the biped

A. Parameters and variables

The model parameters contain the leg length, l, the radius of feet, r, and the distance between the center of circular feet and the ankle, d.

To study the general motion of the biped, four generalized coordinates are used. q_1 is the angle between the stance foot and the vertical line to the horizon. q_2 describes the relative angle made by the stance foot and the stance leg. q_3 indicates the relative angle between the legs, and q_4 denotes the angle between the swing foot and the swing leg.

B. The mathematical model

General equations of motion for passive dynamic walkers is described as follows:

$$\Sigma : \begin{cases} \dot{x} = F(x), & x^- \notin S. \\ x^+ = G(x^-), & x^- \in S. \end{cases} \tag{1}$$

Equation 1 consists of three parts:

1) Vector field F: Describes the system's dynamics between two impacts.
2) Switching surface S: Defines the impact moment.
3) Switching rule G: Relates the states before the impact to states just after that.

Assuming $m/M \to 0$, the equations of motion are derived using Lagrangian mechanics as follows:

$$(2\rho\delta cos(q_1) - 2\rho cos(q_1+q_2) + 2\delta cos(q_2) - \delta^2 - \rho^2 - 1)\ddot{q}_1 - (\delta\, sin(q_1) - sin(q_1+q_2))(1+\rho\dot{q}_1^2) = 0 \tag{2}$$

$$(\rho\, cos(q_1+q_2-q_3) + cos(q_3) - \delta\, cos(q_2-q_3) - 1)\ddot{q}_1 + \ddot{q}_3 - sin(q_1+q_2-q_3) - \dot{q}_1^2(sin(q_3) + \delta\, sin(q_2-q_3)) = 0 \tag{3}$$

where

$$\delta = \frac{d}{l} \quad and \quad \rho = \frac{r}{l}$$

These equations are made dimensionless by scaling time as $t' = t\sqrt{g/l}$.

The switching surface is:

$$\delta\, cos(q_1) - cos(q_1+q_2) + cos(q_1+q_2-q_3) - \delta\, cos(q_1+q_2-q_3-q_4) = 0 \tag{4}$$

Now, by using the angular momentum balancing, the states of system switch into their new values according to the following switching rules:

$$\begin{cases} q_1^+ = q_1^- + q_2^- - q_3^- - q_4^- \\ q_2^+ = q_4^- \\ q_3^+ = -q_3^- \\ q_4^+ = q_2^- \end{cases} \tag{5}$$

$$\mathbf{M}_{2\times2}\begin{pmatrix}\dot{q}_1^+ \\ \dot{q}_3^+\end{pmatrix} = \mathbf{N}_{2\times2}\begin{pmatrix}\dot{q}_1^- \\ \dot{q}_3^-\end{pmatrix} + \mathbf{Z}_{2\times2}\begin{pmatrix}P_x \\ P_y\end{pmatrix} \tag{6}$$

where

$$\begin{aligned} m_{11} &= -2\delta\, cos(q_2^+) - 2\delta\rho\, cos(q_1^+) + 2\rho\, cos(q_1^+ + q_2^+) + \delta^2 + \rho^2 + 1 \\ m_{21} &= \delta\, cos(q_2^+ - q_3^+) - cos(q_3^+) - \rho\, cos(q_1^+ + q_2^+ - q_3^+) + 1 \\ m_{12} &= 0 \qquad m_{22} = -1 \end{aligned}$$

$$\begin{aligned} n_{11} &= cos(q_3^-) - \delta\, cos(q_2^- - q_3^-) + \rho\, cos(q_1^- + q_2^- - q_3^-) - \delta\, cos(q_3^- + q_4^-) + \rho\, cos(q_1^- + q_2^-) + \rho^2 \\ &\quad + \delta^2\, cos(q_3^- - q_2^- + q_4^-) - \rho\delta\, cos(q_1^-) - \delta\rho\, cos(q_1^- + q_2^- - q_3^- - q_4^-) \\ n_{21} &= \delta\, cos(q_2^-) - \rho\, cos(q_1^- + q_2^-) \\ n_{12} &= n_{22} = 0 \end{aligned}$$

$$\begin{aligned} z_{11} &= \delta\, cos(q_1^- + q_2^- - q_3^- - q_4^-) - cos(q_1^- + q_2^- - q_3^-) - \delta\, cos(q_1^-) + cos(q_1^- + q_2^-) \\ z_{12} &= \delta\, sin(q_1^- + q_2^- - q_3^- - q_4^-) - sin(q_1^- + q_2^- - q_3^-) - \delta\, sin(q_1^-) + sin(q_1^- + q_2^-) \\ z_{21} &= \rho - \delta\, cos(q_1^-) + cos(q_1^- + q_2^-) \\ z_{22} &= \rho - \delta\, sin(q_1^-) + sin(q_1^- + q_2^-) \end{aligned}$$

Superscripts "+" and "−" show the states just after and before the impact, respectively. P_x and P_y are the components of the push-off impulse.

All formulations could be replaced by a Poincaré map that relates the states just after the heel-strike to the states just after the next one:

$$X_{i+1} = P(X_i) \tag{7}$$

where X_i demonstrates the states of the system at the beginning of the ith step. When the period-one limit cycle walking exists, the map is given by:

$$X^* = P(X^*) \tag{8}$$

where X^* is the system's fixed point. The Jacobian of Poincaré map at the system's fixed points should be calculated to evaluate the stability. If all the eigenvalues of this Jacobian matrix are within the unit circle in the complex plane, the fixed points are stable; otherwise, the robot's fall is inevitable.

C. Controller design

The concept of VHC is implimented to control the foot during the swing phase kinematically. In this regard, an event-based feedback controller adjusts the heel-strike according to the following constraint:

$$\begin{cases} q_4 & \text{remains unchanged if } \ q_3 \geq \phi \\ q_4 = K(q_3 - q_r) & if \ \ q_3 < \phi \\ q_2 & \text{remains unchanged} \end{cases} \tag{9}$$

where q_r is a reference value, preferred to be equal to q_3^*; representing the absolute value of q_3 at the moment of heel strike when the configuration of biped satisfies $q_2 = q_4 = 0$. Also, ϕ is an arbitrary value defining controller intervention during the swing phase, and K is a constant gain which must be determined.

When the disturbance is included, q_3 will be diverted from its nominal value, so q_4 and then the switching surface changes. Now if an appropriate value of K is chosen, the switching surface will reshape back to its initial state together by eliminating the external disturbance. Note since we do not follow any systematic approach in this study, K must be numerically found.

III. Simulation Results

Numerical techniques are employed to show how RSS can be used to improve the stability of bipedal dynamic walking.

A. Uncontrolled dynamic walking

For a set of specified parameters, $P = 0.01$ and $\delta = \rho = 0.2$, a stable walking cycle is presented in Fig. 2. The figure shows the angles of the robot when it permanently walks on the level ground; where the fixed point is:

$$x_0 = [q_1 \ \ \dot{q}_1 \ \ q_2 \ \ \dot{q}_2 \ \ q_3 \ \ \dot{q}_3 \ \ q_4 \ \ \dot{q}_4] = \\ [0.1143 \ \ -0.1091 \ \ 0 \ \ 0 \ \ 0.2284 \ \ -0.0023 \ \ 0 \ \ 0]$$

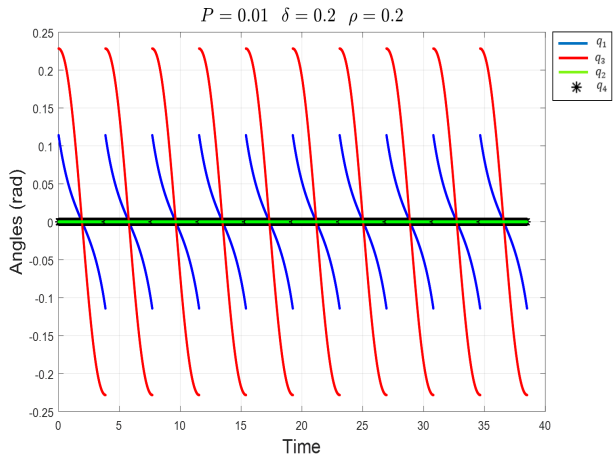

Fig. 2. An example of limit cycle walking for a set of parameters

Fig. 3 shows the values of q_3^* versus push-off; while $\delta = \rho = 0.2$. This figure demonstrates the stable and unstable limit cycles of the system. According to the figure, the biped presents stable period-one limit cycle walking for $P \leq 0.2$. By increasing P, the period-doubling route to chaos occurs. The red line in the figure depicts the unstable limit cycles, which will be stabilized by using RSS.

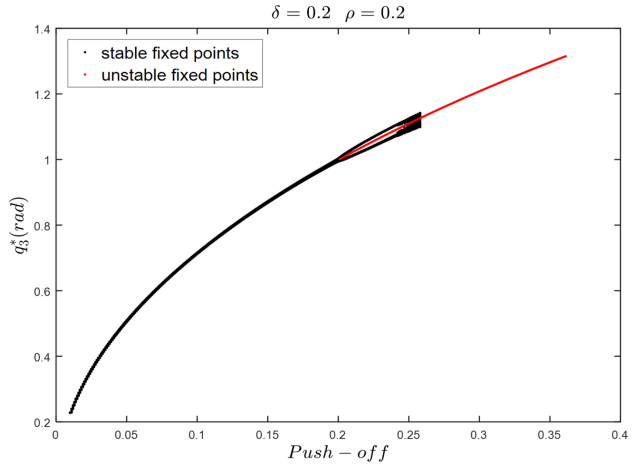

Fig. 3. Stable and unstable limit cycles

B. Controlled dynamic walking

Fig. 4 shows possible values of K, which can be used to stabilize unstable limit cycles. According to Fig. 4, for each value of $P \leq 0.361$, a closed interval of K is fined, which guarantees the stability of the motion. The largest absolute eigenvalue of the Jacobian matrix is also detected by the color bar beside the figure. Fig. 4 reveals that the range of stable motion has been promoted by 80%. Also, because of the massless feet, the efficiency of the gait for each value of P is unvaried, while the stability could be adjusted by changing K. Moreover, it means that the same dynamic walkers with the same step length and step velocity could have different stability condition.

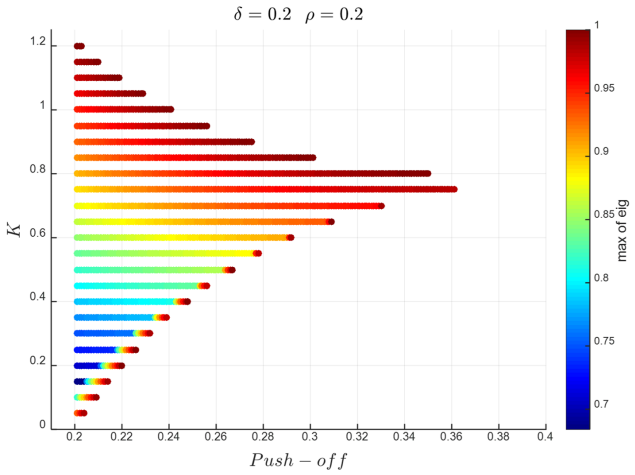

Fig. 4. The unstable region stabilized by RSS.

For three different values of K, the bifurcation diagrams are plotted. Fig. 5 and Fig. 6 show the step length and step velocity versus push-off, respectively. Results show that by increasing K, the robot can stabily take the longer steps at higher speeds. In other words, it would be possible to shift the bifurcation point somewhere forward by regulating the value of the controller's constant, i.e., K.

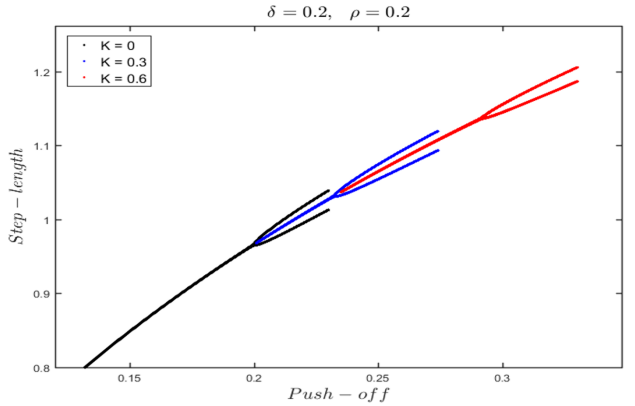

Fig. 5. Step-length versus push-off for three different values of K

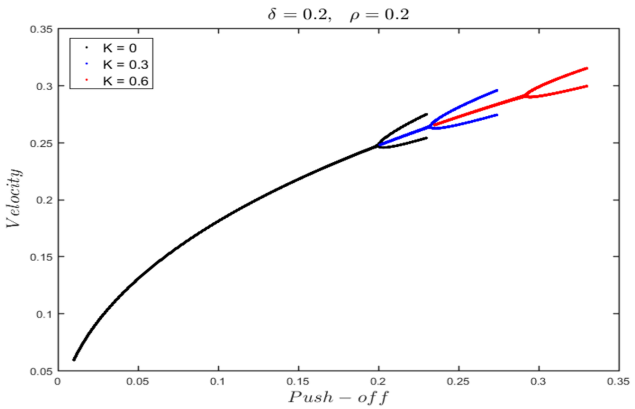

Fig. 6. Velocity versus push-off for three different values of K

IV. CONCLUSIONS AND FUTURE WORKS

In this study, the concept of RSS is examined for the level-ground dynamic walking. It has been shown that this concept can successfully extend the stability of a push-off based dynamic walker. It is also demonstrated that the similar walking trajectories could have entirely different stable condition, while the gait's efficiency is kept unvaried.

In future studies, we plan to model the push-off actuation in detail to take a step towards a real dynamic biped. Furthermore, since the presented biped merely walks based on its natural dynamics, it would be desired to design walking trajectories in advance. In this regard, some theories like foot placement could be helpful.

REFERENCES

[1] M. Vukobratovic and D. Juricic, "contribution to the synthesis of biped gait," IEEE Transactions on Biomedical Engineering, 16(01), pp.1–6, 1969.

[2] M. Vukobratovic and B. Borovac, "Zero-moment point thirty five years of its life," International Journal of Humanoid Robotics, 1(01), pp.157–173, 2004.

[3] D.G.E. Hobbelen and M.Wisse, "Ankle actuation for limit cycle walkers," International Journal of Humanoid Robotics, 27(6), pp. 709–735, 2008.

[4] P.A. Bhounsule, J.Cortell, A. Grewal, B. Hendriksen, J.G.D. Karssen, CH. Paul and A. Ruina, "Low-bandwidth reflex-based control for lower power walking: 65 km on a single battery charge," Int. J. Robot, 33(10), pp. 1305–1321, 2014.

[5] J.H. Solomon, M.Wisse, and M.J.Z. Hartmann, "Fully interconnected, linear control for limit cycle walking," Adaptive Behavior, 18(6), pp. 492–506, 2010.

[6] D.G.E. Hobbelen and M.Wisse, "Active lateral foot placement for 3D stabilization of a limit cycle walker prototype," International Journal of Humanoid Robotics, 6(1), pp. 93–116, 2009.

[7] E. Borzova and Y. Hurmuzlu, "Passively walking five-link robot," Automatica 40(4),pp. 621–629,2004.

[8] A. Goswami, B. Thuilot, B. Espiau, " A study of the passive gait of a compass-like biped robot: Symmetry and chaos," Robot. Res. 17(12),pp. 1282–1301,1998.

[9] M.Wisse, A. Schwab, L. Vander Helm, "Passive dynamic walking model with upper body," Robotica 22(6), pp.681–688, 2004.

[10] M. Wisse, Ch. Atkeson, D. Kloimwieder,"Swing leg retraction helps biped walking stability," Proc. of the IEEE-RAS International Conference on Humanoid Robots, pp. 295–300,2005.

[11] A.T. Safa, S.mohammadi, S.E. Hajmiri, M. Naraghi and A. Alasty, "How local slopes stabilize passive bipedal locomotion?," Mechanism and Machine Theory, 100(1), pp. 63–82, 2016.

[12] A.T. Safa, S. Mohammadi, M. Naraghi, and A. Alasty, "Stability improvement of a dynamic walking system via reversible switching surfaces," Multibody Syst Dyn, 43(4), pp. 349–367, 2018.

[13] M. Maggiore and L. Consolini, "Virtual holonomic constraints for EulerLagrange systems," IEEE Trans. Autom. Control, 58(4), pp. 1001–1008, 2013.

[14] A.S. Shiriaev, L.B. Shiriaev, A. Johansson, and R. Sandberg, "Virtual-holonomic-constraints-based design of stable oscillations of furuta pendulum: theory and experiments," IEEE Trans. Robot, 23(4), pp.827–832, 2007.

[15] L. Freidovich, A. Robertsson, A. Shiriaev, and R. Johansson, "Periodic motions of the pendubot via virtual holonomic constraints: theory and experiments," Automatica, 44(3), pp.785–791, 2008.

[16] M. Montanari, F. Rossi, and C. Tonielli, "Control of a camless engine electromechanical actuator:position reconstruction and dynamic performance analysis," IEEE Trans. Ind. Electron, 51(2), pp.299–311, 2004.

[17] L. Consolini and M. Maggiore, "Control of a bicycle using virtual holonomic constraints," Automatica, 49(9), pp. 2831–2839, 2013.

[18] E.R. Westervelt, J.W. Grizzle, and D.E. Koditschek, "Hybrid zero dynamics of planar biped walkers," IEEE Trans. Autom. Control, 48(1), pp. 42–56, 2003.